

# Generic Contrast Agents

Our portfolio is growing to serve you better. Now you have a *choice*.



[VIEW CATALOG](#)

# AJNR

This information is current as of May 24, 2025.

## **Cerebral Hemodynamics in Moyamoya Disease: Correlation between Perfusion-Weighted MR Imaging and Cerebral Angiography**

O. Togao, F. Mihara, T. Yoshiura, A. Tanaka, T. Noguchi, Y. Kuwabara, K. Kaneko, T. Matsushima and H. Honda

*AJNR Am J Neuroradiol* 2006, 27 (2) 391-397  
<http://www.ajnr.org/content/27/2/391>

ORIGINAL  
RESEARCH

O. Togao  
F. Mihara  
T. Yoshiura  
A. Tanaka  
T. Noguchi  
Y. Kuwabara  
K. Kaneko  
T. Matsushima  
H. Honda

# Cerebral Hemodynamics in Moyamoya Disease: Correlation between Perfusion-Weighted MR Imaging and Cerebral Angiography

**BACKGROUND AND PURPOSE:** In Moyamoya disease, the relationship between cerebral hemodynamics and angiographic findings has not been fully evaluated. The purpose of this study is to evaluate hemodynamics in Moyamoya disease with perfusion-weighted MR imaging (PWI) and cerebral angiography.

**METHODS:** Twenty patients with Moyamoya disease were the subjects. Mean transit time (MTT) derived from PWI was calculated in the medial frontal lobes, the posterior frontal lobes, the occipital lobes, and the basal ganglia. From the angiographies, we classified the degrees of internal carotid artery (ICA) and posterior cerebral artery (PCA) stenoses as well as the degrees of Moyamoya vessels and leptomeningeal anastomosis (LMA). MTT in each region was compared with the angiographic findings.

**RESULTS:** MTT positively correlated with the degree of ICA stenosis in the medial frontal ( $P < .01$ ), posterior frontal ( $P < .001$ ), and occipital ( $P < .001$ ) lobes, as well as in the basal ganglia ( $P < .001$ ). MTT correlated with the degree of PCA stenosis in the medial frontal ( $P < .001$ ), posterior frontal ( $P < .001$ ), and occipital ( $P < .001$ ) lobes, as well as in the basal ganglia ( $P < .001$ ). MTT correlated with the degree of Moyamoya vessels in the medial frontal ( $P < .05$ ) and posterior frontal ( $P < .01$ ) lobes. A multivariate analysis revealed that ICA and PCA stenoses and Moyamoya vessels were independent factors that prolonged MTT.

**CONCLUSION:** Both ICA and PCA stenoses may influence overall cerebral perfusion in Moyamoya disease. The development of Moyamoya vessels may indicate hemodynamic impairment.

Moyamoya disease is a rare cerebrovascular occlusive disorder most often found among the Japanese.<sup>1-3</sup> This disease is angiographically defined as progressive steno-occlusion of the bilateral internal carotid arteries (ICAs) with characteristic abnormal vascular networks, so-called Moyamoya vessels, at the base of the brain.<sup>1-3</sup> Hemodynamics in Moyamoya disease are rather complex. Steno-occlusive change can occur not only in the ICA but also in the posterior cerebral artery (PCA).<sup>4,5</sup> Leptomeningeal anastomosis (LMA) from posterior circulation and transdural anastomosis from the external carotid artery (ECA), as well as Moyamoya vessels, could develop to supply the ischemic brain.<sup>1,2,5</sup> The importance of posterior circulation in Moyamoya disease has recently become recognized.<sup>6-8</sup> Only a few reports have investigated the relationship between cerebral angiography findings and hemodynamic status in Moyamoya disease.<sup>6-8</sup> By using dynamic susceptibility contrast perfusion-weighted MR imaging (DSC-PWI), Yamada et al demonstrated that PCA steno-occlusive change was significantly related to cerebral hemodynamics in Moyamoya patients but ICA was not.<sup>6</sup>

In Moyamoya disease, as in other chronic steno-occlusive cerebrovascular diseases, the steno-occlusive change in the main cerebral arteries decreases the cerebral perfusion pressure (CPP), and collateral circulation maintains cerebral blood flow (CBF).<sup>9,10</sup>

The mean transit time (MTT) and its reverse ratio have been used as indices for CPP in focal ischemia.<sup>11,12</sup> Quantitative mea-

surement of the MTT by using a deconvolution algorithm can be a sensitive and reliable indicator of the cerebral perfusion reserve capacity, and it provides important information for the management of patients with occlusive cerebrovascular diseases.<sup>13-15</sup>

We evaluated the relationship between angiographic findings and the regional MTT obtained by DSC-PWI in 20 patients with Moyamoya disease.

## Subjects and Methods

### Patients

From September 1995 to March 2004, a total of 29 patients with Moyamoya disease were studied by both DSC-PWI and cerebral angiography in our radiology department. Of these 29 patients, we excluded 3 patients who had previously undergone intracranial-extracranial revascularization surgery and 3 patients for whom the interval between PWI and cerebral angiography was longer than 3 months. One patient who had an extensive infarcted lesion ( $>8$  cm in diameter) in the left hemisphere on MR imaging was also excluded. The remaining 20 patients were included in this study. The diagnosis of Moyamoya disease was made by the angiographic appearance of ICA stenosis or occlusion and characteristic collateral arteries, so-called Moyamoya vessels, at the base of the brain. The patients included 7 men and 13 women ranging in age from 5 to 48 years (mean  $\pm$  SD,  $22.3 \pm 14.1$  years). The subjects' clinical types were as follows: transient ischemic attack (TIA) type, 15 patients; hemorrhagic type, 4 patients; asymptomatic type, one patient. The interval between PWI and cerebral angiography was  $18 \pm 30$  days (range, 0–89 days). In all patients, clinical status had been stable throughout the period between PWI and cerebral angiography, and no new stroke or exacerbation of TIA had occurred in that period. Informed consent was obtained from each patient and his or her family. This study was approved by our institutional review board. The clinical features and radiologic findings of the subjects are summarized in Table 1.

Received May 2, 2005; accepted after revision July 8.

From the Department of Clinical Radiology (O.T., F.M., T.Y., A.T., T.N., Y.K., K.K., H.H.), Graduate School of Medical Sciences, Kyushu University, and the Department of Neurosurgery (T.M.), Hamanomachi Hospital, Fukuoka, Japan.

Address correspondence to Futoshi Mihara, MD, PhD, Department of Clinical Radiology, Graduate School of Medical Sciences, Kyushu University, Maidashi 3-1-1, Higashi-ku, Fukuoka 812-8582, Japan.

**Table 1: Clinical data and image findings**

Patient No./ Age (y)/Sex	Clinical Type	Major Clinical Symptoms	Duration from Onset of Disease	Duration from Last TIA	Infarct or Hemorrhage on MRL Image
1/5/M	TIA	Weakness of bilateral limbs	11 mo	2 mo	Negative
2/6/F	TIA	Weakness of left limbs	1 y	3 mo	Negative
3/7/F	TIA	Involuntary movement of right hand	10 mo	1 w	Negative
4/9/F	TIA	Weakness of right limbs	2 y	3 mo	Bilateral frontoparietal cortex
5/10/M	TIA	Weakness of right hand	5 mo	5 mo	Negative
6/10/F	TIA	Weakness of left hand	5 y	4 mo	Negative
7/11/F	TIA	Weakness of right limbs	1 y	1 mo	Left frontal cortex, left basal ganglia
8/13/M	TIA	Weakness of bilateral lower limbs	10 y	4 mo	Right frontal white matter
9/15/M	TIA	Weakness of bilateral limbs	7 y	1 y	Right frontal cortex
10/17/M	TIA	Weakness of bilateral limbs	5 y	1 w	Negative
11/17/F	TIA	Weakness of right limbs	3 y	1 mo	Left frontotemporoparietal white matter
12/26/M	H	Headache	21 y	—	Bilateral frontoparietal white matter
13/28/F	TIA	Weakness of bilateral limbs	14 y	1 mo	Negative
14/31/F	H	Weakness of right hand	3 y	—	Left basal ganglia
15/34/F	None	Hemorrhage of bilateral ocular fundus	7 y	—	Negative
16/36/F	TIA	Weakness of right limbs	2 mo	2 mo	Left frontal cortex, left basal ganglia
17/37/F	TIA	Weakness of right hand	6 mo	1 mo	Left frontoparietal white matter
18/41/F	H	Headache	4 mo	—	Right temporal subcortex
19/45/F	H	Headache	3 mo	—	Right thalamus
20/48/M	TIA	Weakness of bilateral limbs	22 y	1 wk	Left frontal cortex, right basal ganglia

**Note.**—TIA indicates transient ischemic attack; H, hemorrhagic.

### Dynamic Susceptibility Contrast-Enhanced MR Imaging Protocol

Dynamic susceptibility contrast-enhanced MR imaging studies were performed with a 1.5T MR unit, Magnetom Vision (Siemens Medical Systems, Erlangen, Germany), by using a single-shot gradient-echo type of echo-planar sequence with a standard head coil. The imaging parameters were as follows: TE = 54 milliseconds; flip angle = 90°; acquisition matrix = 128 × 128; field of view = 230 × 230 mm; and section thickness = 5 mm. Gadopentetate dimeglumine at 0.05 mmol/kg body weight was administered as a bolus through the antecubital vein at a rate of 2 mL/s, followed by a 20-mL saline flush.<sup>12,14</sup> The contrast agent was injected manually. A single axial plane at the level of the striatum was scanned every 1 second, from 10 seconds before to 50 seconds after contrast injection. To allow for equilibration of image magnetization, the first 3 images were excluded from the data analysis. T1-weighted images, T2-weighted images, and MR angiographies were also obtained.

### MR Imaging Data Analysis

All DSC MR imaging data were transferred to a Linux workstation, and images of the perfusion parameters were generated by using the image-analytical program of Dr. View/Linux (Asahi Kasei Joho System Co., Tokyo, Japan). First, smoothing of the MR images was performed with a 5 mm × 5 mm uniform smoothing kernel before the data analysis. The maximum concentration was calculated pixel by pixel before arterial input function (AIF) sampling.<sup>16</sup> To reduce the partial volume effect, only pixels with a signal intensity–intensity reduction of >99.5% of the maximum value were extracted automatically in each region of interest. The mean concentration time curve of these pixels was then used to determine the AIF, which was obtained from circular regions of interest (2 mm in diameter) placed manually on the ipsilateral middle cerebral artery (MCA) or PCA branch at the level of the basal ganglia. The MTT calculation is highly dependent on the choice of AIF. We therefore measured AIF from the MCA to calculate MTT in the anterior circulation territory, and AIF from the PCA to calculate MTT in the posterior circulation territory (Fig 1A).<sup>17</sup>

The signal intensity in each voxel in the brain parenchyma was

converted to transverse relaxation rate. The signal intensity time curves  $S(t)$  were then converted into concentration time curves ( $C_m(t)$ ) on a pixel-by-pixel basis by using the following equation:

$$1) \quad C_m(t) = -\ln\left(\frac{S(t)}{S_0}\right)/TE,$$

where  $S_0$  denotes the precontrast baseline signal intensity,  $S(t)$  is the signal intensity at time  $t$  after injection of the contrast agent, and TE is the echo time.  $C_m(t)$  was then deconvoluted with AIF [ $C_a(t)$ ] by using a fast Fourier transformation, and  $C(t)$  was obtained. This approach has been described in detail by Wirestam et al<sup>18</sup> and Ostergaard et al.<sup>19</sup>

The cerebral blood volume (CBV) was calculated by the following equation:

$$2) \quad CBV = \frac{k_H \int_0^\infty C_m(t) dt}{\rho \int_0^\infty C_a(t) dt},$$

where  $\rho$  is the attenuation of the brain tissue ( $\rho = 1.04 \text{ g/cm}^3$ ) and  $k_H$  (0.73) is a factor correcting for the difference in hematocrit between the capillaries ( $H_{\text{cap}} = 0.25$ ) and the large arterial vessels ( $H_{\text{art}} = 0.45$ ).<sup>20</sup> The CBF was calculated as

$$3) \quad CBF = \frac{k_H}{\rho} C_{\text{max}},$$

where  $C_{\text{max}}$  is the peak height of  $C(t)$ . In addition to the AIF, the venous output function (VOF) was obtained from regions of interest placed on the superior sagittal sinus, which is large enough to allow for VOF sampling without a partial volume effect.<sup>21,22</sup> The VOF was used to correct for partial volume effects in the AIF due to the relatively small caliber of the MCA or PCA. This VOF correction was performed by multiplying the AIF with  $\int \text{AIF} / \int \text{VOF}$ .<sup>22</sup> The MTT was calculated based on the ratio of CBV/CBF in the PWI.

$$4) \quad MTT = \frac{CBV}{CBF}.$$

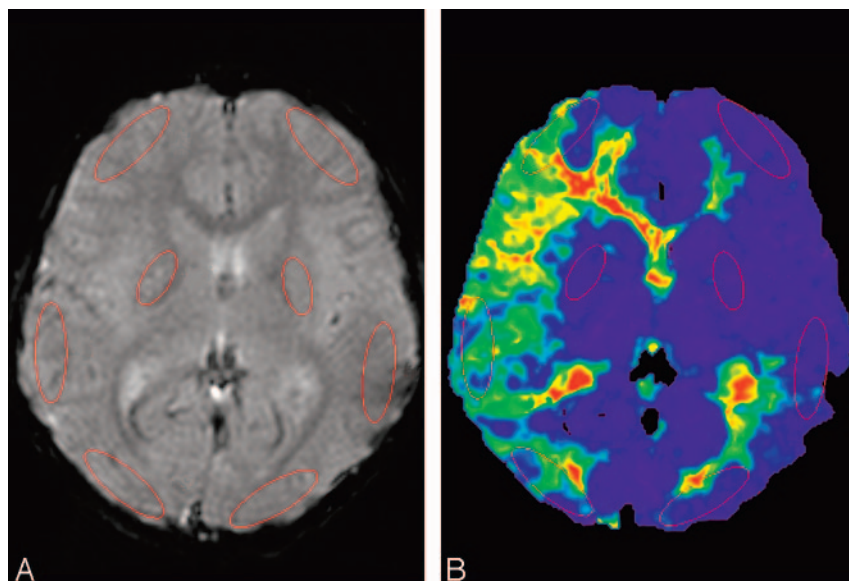


**Fig 1.** Regions of interest drawn in a PWI (A) and MTT map (B). The regions of interest were placed on cortical regions in the medial frontal lobe in the ACA distribution, in the posterior frontal lobe in the MCA distribution and in the occipital lobes in the PCA distribution as well as in the putamen in each cerebral hemisphere. To calculate the MTTs in the frontal lobes, as well as in the basal ganglia, an AIF (blue dot) was obtained from an ipsilateral MCA branch to represent anterior circulation. In calculating MTT in the occipital lobe, an AIF (yellow dot) was obtained from an ipsilateral PCA branch. This MTT map (B) was calculated with the AIF obtained from the right MCA branch.

Kaneko et al demonstrated that CBF and CBV obtained by the same method as ours were significantly higher than those obtained by  $^{15}\text{O}$ -positron-emission tomography (PET).<sup>14</sup> In their study, the normalization factors between PWI and  $^{15}\text{O}$ -PET were estimated as 0.73 for CBF and 0.49 for CBV in the gray matter.<sup>14</sup> Therefore, we also apply this normalization factor in the calculation of MTT.

The regions of interest were placed on cortical regions in the medial frontal lobes in the anterior cerebral artery (ACA) distribution, in the posterior frontal lobes in MCA distribution, and in the occipital lobes in PCA distribution as well as in the putamen in each cerebral hemisphere (Fig 1). The regions of interest in the cortical regions were  $35 \times 10$  mm in diameter, and those in the putamen were  $20 \times 10$  mm. Areas of infarction were not included in these regions of interest.

### Cerebral Angiography

The cerebral angiography was performed by using a system of stereoscopic biplane digital subtraction angiography (DFP-200A; Toshiba Medical Systems, Tokyo, Japan). In all 20 patients, angiograms of bilateral ICAs and ECAs, as well as unilateral or bilateral vertebral arteries (VAs), were obtained by using the transfemoral Seldinger's catheterization technique. A dose of about 10 mL of ioxaglate was injected into each vessel. Two board-certified radiologists (T.Y. and O.T.), who were blinded to the patients' clinical information and MR findings, met and discussed their findings of the cerebral angiographies on the printed films and reached a consensus for each film. According to the resulting consensus findings of cerebral angiography of 40 hemispheres in the 20 patients, we applied a staging system to determine the degrees of steno-occlusive vascular change for both anterior and posterior circulation. The degree of the development of Moyamoya vessels at the base of the brain and that of leptomeningeal collateral vessels were also evaluated. We classified steno-occlusive lesions of the distal ICA as well as those of the proximal regions of both ACA and MCA into 6 angiographic stages, adapted from Suzuki's classification<sup>1,2</sup>: stage 1, mild narrowing of the carotid artery bifurcation only ( $<50\%$  reduction in diameter); stage 2, moderate to severe stenosis of the carotid artery bifurcation ( $\geq 50\%$  reduction in diameter); stage 3, partial disappearance of the terminal segment of the ICA and of the proximal regions of the ACA and MCA; stage 4, occlusion of the ICA bifurcation, the main trunk of the ACA, and the MCA left faint traces within the Moyamoya vessels at the base

of the brain; stage 5, occlusion of the ICA bifurcation and absence of the ACA and MCA, but subtle anterograde blood flow to ACA and MCA branches through the basal Moyamoya vessels remained; stage 6, complete occlusion of the ICA and disappearance of all ACA and MCA branches. We also staged PCA steno-occlusive lesions into 4 stages: stage 1, no occlusive change in the PCA; stage 2, mild stenosis ( $<50\%$  reduction in diameter) of the PCA with good visualization of distal branches; stage 3, moderate to severe ( $\geq 50\%$  reduction in diameter) stenosis of the PCA with poor visualization of distal branches; stage 4, occlusion of the PCA with almost no visualization of distal branches. The development of basal Moyamoya vessels was also graded into 4 stages: stage 1, no Moyamoya vessels were seen; stage 2, Moyamoya vessels were localized in the area around the ICA bifurcation, and each vessel was fine and had little contrast; stage 3, Moyamoya vessels had intermediate extension and thickness; stage 4, Moyamoya vessels extended a great deal and each one was thick and strongly opacified. The degree of development of the leptomeningeal collateral circulation to ICA distribution from the PCA and from the posterior pericallosal arteries was classified into 4 grades: stage 1, no leptomeningeal collateral circulation; stage 2, leptomeningeal cortical branches were found in one of 3 lobes; stage 3, collateral arteries extended to 2 of 3 lobes; stage 4, leptomeningeal collateral arteries extended to all 3 lobes.

### Statistical Analysis

We evaluated the relationship between each region of interest's MTT and each angiographic finding by using univariate and multivariate analyses. The univariate analyses of the relationship between each region of interest's MTT and the angiographic stages of ICA, PCA, development of Moyamoya vessels, and LMA were performed by using the Spearman rank correlation test. Multiple linear regression was used in the multivariate analysis. The multivariate analysis model included all angiographic factors (stages of ICA, PCA, Moyamoya vessels, and LMA), patient age, and clinical type (TIA type = 1, hemorrhagic type = 2). A  $P$  value  $< .05$  was considered statistically significant in this study. All statistical analyses were performed with StatView version 5.0 (SAS Institute Inc., Cary, NC).

### Results

The stage distribution of stenotic or occlusive lesions in the ICA system of the 40 hemispheres was as follows: stage 1, 6 hemispheres; stage 2, 3 hemispheres; stage 3, 9 hemispheres; stage 4, 13 hemispheres; stage 5, 6 hemispheres; stage 6, 3 hemispheres. Of the 20 patients, 5 (25%) were found to have steno-occlusive lesions in one or both PCAs. Eight PCAs (20%) of the 40 sides showed steno-occlusive change. The

**Table 2: Mean MTT in each region and ICA stage**

	ICA Stage						<i>r</i>
	1 ( <i>n</i> = 6)	2 ( <i>n</i> = 3)	3 ( <i>n</i> = 9)	4 ( <i>n</i> = 13)	5 ( <i>n</i> = 6)	6 ( <i>n</i> = 3)	
Medial frontal	9.1 ± 3.1	10.8 ± 2.1	11.6 ± 2.9	13.8 ± 6.1	17.4 ± 3.3	14.7 ± 2.4	.52 <sup>†</sup>
Posterior frontal	8.6 ± 2.6	8.7 ± 1.0	11.8 ± 5.1	14.1 ± 5.0	20.0 ± 5.7	16.1 ± 4.8	.64 <sup>‡</sup>
Occipital	9.3 ± 2.8	9.3 ± 1.0	10.8 ± 2.6	11.7 ± 3.3	18.9 ± 2.9	15.4 ± 6.3	.58 <sup>‡</sup>
Basal ganglia	8.6 ± 2.8	7.4 ± 1.1	9.6 ± 2.9	10.7 ± 3.5	15.1 ± 3.8	14.4 ± 2.5	.58 <sup>‡</sup>

**Note.**—MTT indicates mean transit time; ICA, internal carotid artery.

<sup>\*</sup>, *P* < .05; <sup>†</sup>, *P* < .01; <sup>‡</sup>, *P* < .001; based on Spearman rank correlation test.

**Table 3: Mean MTT in each region and PCA stage**

	PCA Stage				<i>r</i>
	1 ( <i>n</i> = 32)	2 ( <i>n</i> = 1)	3 ( <i>n</i> = 5)	4 ( <i>n</i> = 2)	
Medial frontal	11.9 ± 4.5	16.4	16.7 ± 2.6	20.2 ± 2.2	.56 <sup>†</sup>
Posterior frontal	11.5 ± 4.3	23.1	19.0 ± 4.6	24.6 ± 2.0	.60 <sup>‡</sup>
Occipital	10.7 ± 2.8	14.5	18.0 ± 3.1	22.6 ± 0.2	.64 <sup>‡</sup>
Basal ganglia	9.8 ± 3.2	14.4	13.1 ± 2.4	19.6 ± 1.0	.53 <sup>‡</sup>

**Note.**—MTT indicates mean transit time; PCA, posterior cerebral artery.

<sup>\*</sup>, *P* < .05; <sup>†</sup>, *P* < .01; <sup>‡</sup>, *P* < .001; based on Spearman rank correlation test.

**Table 4: Mean MTT in each region and stage of Moyamoya vessels**

	Moyamoya Vessels				<i>r</i>
	1 ( <i>n</i> = 9)	2 ( <i>n</i> = 22)	3 ( <i>n</i> = 5)	4 ( <i>n</i> = 4)	
Medial frontal	11.0 ± 3.7	12.4 ± 3.7	14.6 ± 7.9	19.0 ± 2.5	.35 <sup>*</sup>
Posterior frontal	11.3 ± 4.5	11.6 ± 3.8	16.4 ± 7.1	24.1 ± 1.5	.47 <sup>†</sup>
Occipital	12.0 ± 4.2	11.3 ± 3.8	13.2 ± 6.0	17.3 ± 3.8	.24
Basal ganglia	10.5 ± 3.5	10.2 ± 3.1	11.3 ± 6.6	14.7 ± 3.1	.15

**Note.**—MTT indicates mean transit time.

<sup>\*</sup>, *P* < .05; <sup>†</sup>, *P* < .01; <sup>‡</sup>, *P* < .001; based on Spearman rank correlation test.

**Table 5: Mean MTT in each region and stage of leptomeningeal anastomosis**

	LMA				<i>r</i>
	1 ( <i>n</i> = 4)	2 ( <i>n</i> = 8)	3 ( <i>n</i> = 8)	4 ( <i>n</i> = 20)	
Medial frontal	15.4 ± 5.8	13.0 ± 5.6	12.5 ± 5.3	12.8 ± 4.1	−.05
Posterior frontal	16.2 ± 10.0	15.1 ± 6.5	11.3 ± 4.4	13.0 ± 4.9	−.10
Occipital	15.3 ± 8.9	14.9 ± 5.2	10.7 ± 2.1	11.3 ± 2.9	−.22
Basal ganglia	13.7 ± 7.4	11.6 ± 3.4	9.5 ± 2.8	10.5 ± 3.3	−.16

**Note.**—MTT indicates mean transit time; LMA, leptomeningeal anastomosis.

<sup>\*</sup>, *P* < .05; <sup>†</sup>, *P* < .01; <sup>‡</sup>, *P* < .001; based on Spearman rank correlation test.

stage distribution of the 40 PCAs of the 20 patients was as follows: stage 1, 32 arteries; stage 2, 1 artery; stage 3, 5 arteries; and stage 4, 2 arteries. The grade distribution of the Moyamoya vessels was as follows: stage 1, 9 hemispheres; stage 2, 22 hemispheres; stage 3, 5 hemispheres; and stage 4, 4 hemispheres. The grade distribution of the leptomeningeal vessels was as follows: stage 1, 4 hemispheres; stage 2, 8 hemispheres; stage 3, 8 hemispheres; stage 4, 20 hemispheres.

The results of the univariate analysis of the PWI data and angiographic findings were as follows: MTT significantly correlated with the degree of ICA stenosis in the medial frontal ( $r = 0.52$ ;  $P < .01$ ), posterior frontal ( $r = 0.64$ ;  $P < .001$ ), and occipital ( $r = 0.58$ ;  $P < .001$ ) lobes as well as in the basal ganglia ( $r = 0.58$ ;  $P < .001$ ) (Table 2). MTT also correlated with the degree of PCA stenosis in the medial frontal ( $r = 0.56$ ;  $P < .001$ ), posterior frontal ( $r = 0.60$ ;  $P < .001$ ), and occipital ( $r = 0.64$ ;  $P < .001$ ) lobes as well as in the basal ganglia ( $r = 0.53$ ;  $P < .001$ ) (Table 3). The higher the degree of ICA and PCA stenosis, the longer MTT was. MTT obtained in the medial frontal ( $r = 0.35$ ;  $P < .05$ ) and posterior frontal ( $r = 0.47$ ;

**Table 6: Standard regression coefficient relating to MTT in each region**

	Medial Frontal	Posterior Frontal	Occipital	Basal Ganglia
ICA	0.47 <sup>†</sup>	0.57 <sup>‡</sup>	0.58 <sup>‡</sup>	0.55 <sup>‡</sup>
PCA	0.50 <sup>†</sup>	0.66 <sup>‡</sup>	0.78 <sup>‡</sup>	0.59 <sup>‡</sup>
Moyamoya vessels	0.46 <sup>†</sup>	0.62 <sup>‡</sup>	0.32 <sup>*</sup>	0.28
LMA	−0.12	−0.19	−0.35 <sup>*</sup>	−0.23
Age	0.23	0.15	0.37 <sup>*</sup>	0.38 <sup>*</sup>
Clinical type	−0.01	−0.04	0.25	0.14
R <sup>2</sup>	0.45 <sup>†</sup>	0.70 <sup>‡</sup>	0.73 <sup>‡</sup>	0.52 <sup>†</sup>

**Note.**—MTT indicates mean transit time; ICA, internal carotid artery; PCA, posterior cerebral artery; LMA, leptomeningeal anastomosis.

<sup>\*</sup>, *P* < .05; <sup>†</sup>, *P* < .01; <sup>‡</sup>, *P* < .001; based on multiple linear regression analysis.

$P < .01$ ) lobes was significantly positively correlated with the degree of Moyamoya vessels (Table 4). There was no correlation between the degree of LMA and MTT obtained in each region (Table 5).

The results of the multiple linear regression analysis are summarized in Table 6. It was revealed that both the ICA and PCA



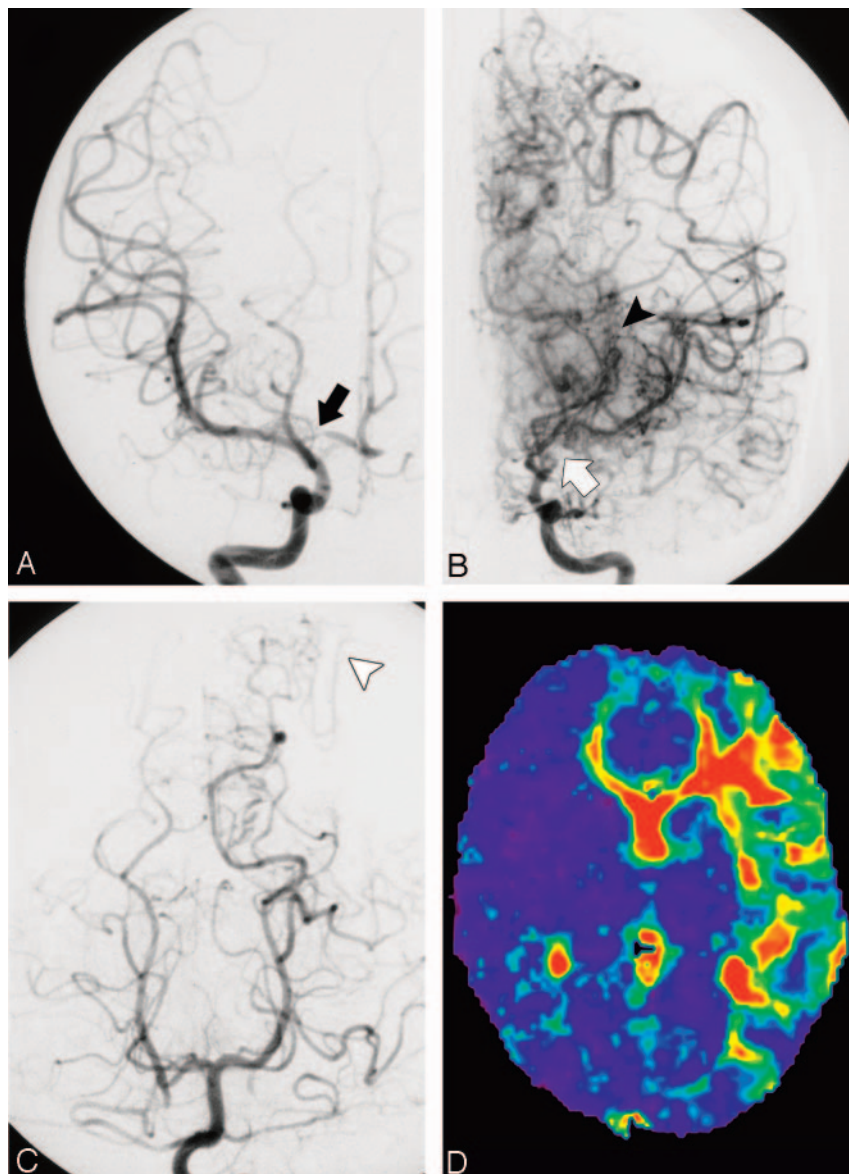


**Fig 2.** A 10-year-old boy with Moyamoya disease who presented with weakness of the right upper extremity. Right internal carotid arteriogram in posterior-anterior projection (A) shows that the right proximal anterior cerebral artery is mildly stenotic (black arrow). No steno-occlusive change is found in the ICA or MCA. The right ICA is in stage 1. No Moyamoya vessels are seen. Left internal carotid arteriograms in posterior-anterior projection (B) show that the right distal ICA and the anterior and MCAs are occluded (white arrow). The left ICA is in stage 3. Marked Moyamoya vessels are seen, and peripheral branches of the anterior cerebral artery and MCA are opacified via the collateral vessels (black arrowhead). On the left vertebral arteriogram in posterior-anterior projection (C), no steno-occlusive change is found in the bilateral posterior cerebral artery. The bilateral posterior cerebral artery is in stage 1. Leptomeningeal collateral vessels from the left posterior cerebral artery to the anterior circulation are seen (white arrowhead). MTT map (D) shows the areas of prolonged mean MTT in the left frontal and temporal lobes. This map was calculated with the AIF obtained from a right MCA branch.

stages were independent significant factors that influenced MTT in each of the 4 regions. The degree of Moyamoya vessels was a significant factor for MTT in the medial and posterior frontal lobes, and occipital lobes. The degree of LMA was a negative significant factor for MTT in the occipital lobe. The patient's age was a positive significant factor for MTT in the occipital lobe and basal ganglia. Clinical type was not significant in any region. Multicollinearity was not observed in any multivariate analysis.

Two representative cases are shown in Figs 2 and 3.

## Discussion

Cerebral hemodynamics in Moyamoya disease have been studied by using PET. According to those reports, patients with Moyamoya disease have reduced CBF and  $\text{CO}_2$  response, and increased CBV, MTT, and oxygen extraction fraction (OEF).<sup>23,24</sup> These hemodynamic changes in Moyamoya disease were explained by decreases in CPP and associated vasodilation. Schumann et al<sup>11</sup> and Gibbs et al<sup>25</sup> demonstrated that, in patients with chronic cerebrovascular occlusive disease, CBF/CBV, an inverse equation of MTT, reflects the local CPP and is correlated with OEF. Kuwabara et al reported that

MTT was prolonged in both pediatric and adult patients with Moyamoya disease and that MTT was related to  $\text{CO}_2$  response.<sup>23,24,26</sup> By using PET, Taki et al found decreased CBF/CBV in patients with Moyamoya disease.<sup>10</sup> PET-obtained MTT has been considered a reliable parameter for evaluating the hemodynamic status of patients with Moyamoya disease.

MTT obtained by PWI has also been used to evaluate the hemodynamic status of patients with occlusive cerebrovascular diseases.<sup>12,14</sup> There are 2 major methods of measuring MTT by using PWI. One is the deconvolution method,<sup>13-16,18,19</sup> and the other is the normalized first moment method.<sup>12,14,15,27</sup> MTT values obtained by deconvolution analysis were reported to be reliable parameters of cerebral hemodynamics.

Kaneko et al reported that MTT obtained by the deconvolution method correlated well with the MTT obtained by  $^{15}\text{O}$ -PET.<sup>14</sup> The deconvolution method requires the AIF obtained from the major cerebral arteries.<sup>19</sup> A crucial problem in Moyamoya disease, however, is the difficulty of obtaining the AIF because of its extensive obstruction around the circle of Willis. The normalized first moment method has been the classic technique to measure MTT by using PWI without AIF; however, MTT determined by the normalized first moment method is distinct from the ideal MTT, because this method is influenced by both the ideal MTT and the first moment of the AIF.<sup>12</sup>

In the present study, the univariate analysis showed that MTT in the medial and posterior frontal lobes, and occipital lobes, as well as that in the basal ganglia, significantly positively correlated with the degrees of both ICA and PCA steno-occlusion. Multiple linear regression analysis revealed that the degrees of both ICA and PCA stages were the independent significant factors that determined the local hemodynamic status in all 4 regions of interest. We speculate that, in Moyamoya disease, cerebral perfusion decreases as both ICA and PCA

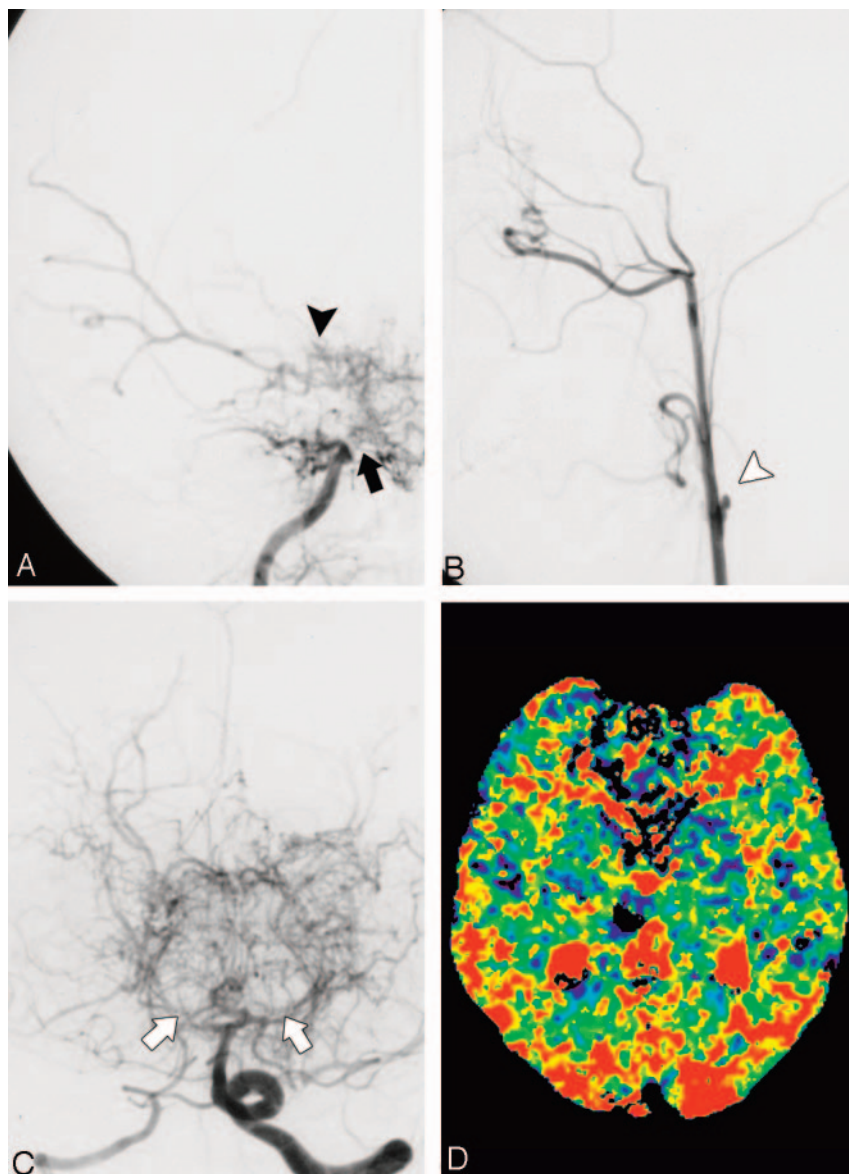


**Fig 3.** A 45-year-old woman with Moyamoya disease who presented with right thalamic hemorrhage. Right internal carotid arteriograms in posterior-anterior projection (A) demonstrated that the right ICA, anterior cerebral artery, and proximal MCA are occluded (large black arrow). The right ICA is in stage 4. Slightly developed Moyamoya vessels are seen around the distal ICA (black arrowhead). The distal MCA is visualized through the Moyamoya vessels. Left common carotid arteriogram in lateral projection (B) shows that the left ICA is completely occluded in its proximal portion (white arrowhead). The left internal ICA is in stage 6. Left vertebral arteriogram in posterior-anterior projection (C) shows severe stenosis in the bilateral posterior cerebral arteries (white arrows). Moyamoya vessels are seen in the posterior region of the brain base. Peripheral branches of bilateral posterior cerebral arteries are visualized through Moyamoya vessels. The bilateral posterior cerebral artery is in stage 3. MTT map (D) demonstrates extensive areas of prolonged MTT in bilateral cerebral hemispheres. This map was calculated with the AIF obtained from a right MCA branch.

stenoses progress. The importance of posterior circulation in Moyamoya disease has been reported.<sup>6-8</sup> Posterior circulation is significant because PCA is thought to play an important collateral role in patients with ICA steno-occlusion, including Moyamoya patients.<sup>6-8</sup> In Moyamoya disease, PCA involvement would occur at the relatively high ICA stages.<sup>6-8</sup> Therefore, as the disease progresses, overall cerebral perfusion would decrease because both anterior and posterior circulation deteriorates. Our results exemplify this theory. Using PWI, Yamada et al demonstrated that the  $\Delta R2^*$  peak value ratio in the cerebral hemisphere decreased and that the  $\Delta R2^*$  peak time ratio increased significantly with the progression of PCA steno-occlusion.<sup>6</sup> Their results are in accordance with our study. In the studies of Yamada et al, however, no correlation was observed between these perfusion parameters and the degree of ICA steno-occlusion, which contradicts our results. One of the reasons for the discrepancy between our study and theirs could be the difference in the parameters used in the evaluation. MTT obtained by the deconvolution method, which we used in our study, would be more sensitive to hemodynamic status than the simple parameters used in their study.

Mugikura et al reported that progressive changes in both the anterior and posterior circulation are associated with the distribution and extent of cerebral infarction on CT or MR.<sup>8</sup> Although the relationship between the infarction and the cerebral hemodynamic status may not be simple, the results of Mugikura et al seem to be consistent with ours.

In the present study, the MTT was significantly prolonged with the development of Moyamoya vessels in the medial and posterior frontal lobes, and occipital lobes. Piao et al reported that the extensive development of basal Moyamoya vessels is a sign of severe hemodynamic impairment in adult patients with ischemic Moyamoya disease.<sup>9</sup> Moyamoya vessels would develop to compensate for the misery cerebral perfusion. We suppose the reason why LMA is insignificant is that, as PCA stenosis advances, the LMA from posterior to anterior circulation decreases, and thus a linear relationship between LMA and MTT would not be obtainable.

Perfusion-weighted MR imaging in Moyamoya disease has potential intrinsic limitations. The presence of steno-occlusion of the main cerebral arteries and collateral vessels always leads to the delay and dispersion of the bolus of the contrast



agent. Calamante et al reported that, in Moyamoya patients, the maps generated with the use of deconvolution can be misleading, resulting in overestimation of the MTT.<sup>29</sup> They mentioned that the main problem is the impossibility of measuring the true AIF, which is generally estimated from a large artery that, in practice, may be distant from the tissue that is being studied. We used the AIF obtained from an MCA or PCA branch at the level of the basal ganglia, which is fine and narrow in patients with Moyamoya disease, and thus the AIF would be susceptible to signal intensity noise and technical error. A new method that can compensate for or resolve this problem is desirable. The other problem is that, in chronic steno-occlusive disease, the reliability of MTT obtained by the deconvolution method has not been fully evaluated in Moyamoya disease, though it has been confirmed to a certain extent in chronic steno-occlusive disease.<sup>13,14</sup> We should have used the ratio or the difference between affected region and normal tissue as a parameter that estimates regional cerebral perfusion. In Moyamoya disease, however, because both cerebral hemispheres are extensively affected, we could not obtain such values.

Our study has several other limitations. Hemodynamic parameters are known to change with age.<sup>23</sup> In Moyamoya disease, clinical presentation differs between adults and pediatric patients.<sup>23</sup> In the results of our multivariate analysis, MTT tended to be prolonged in older patients (Table 6). It would have been better if this study had discussed pediatric and adult patients in separate groups. Another limitation is that the injection of the contrast agent for PWI was performed manually, though at a relatively constant rate that was easily reproducible. Also, transdural collateral vessels from the external carotid artery system, which play an important role in collateral circulation in Moyamoya disease, were not evaluated angiographically. This was because transdural anastomosis is so multifarious that it was not easy to adapt a staging system to these angiographic findings.

## Conclusion

The univariate and multivariate analyses demonstrated that the degrees of both ICA and PCA steno-occlusive change were significant factors in the prolongation of MTT in all 4 cerebral regions measured in patients with Moyamoya disease. These results suggested that both ICA and PCA stenoses influence the global cerebral perfusion in Moyamoya disease. In the multivariate analysis, the degree of Moyamoya vessels was a significant factor in the prolongation of MTT in the medial and posterior frontal and occipital regions. The development of Moyamoya vessels would indicate hemodynamic impairment.

## Acknowledgments

This work was supported in part by a grant-in-aid for scientific research (C2-16591211) from the Japan Society for the Promotion of Science.

## References

- Suzuki J, Takaku A. Cerebrovascular "moyamoya" disease: disease showing abnormal net-like vessels in base of brain. *Arch Neurol* 1969;20:288-99
- Suzuki J, Kodama N. Moyamoya disease: a review. *Stroke* 1983;14:104-10
- Nishimoto A, Takeuchi S. Abnormal cerebrovascular network related to the internal carotid arteries. *J Neurosurg* 1968;29:255-60
- Miyamoto S, Kikuchi H, Karasawa J, et al. Study of the posterior circulation in moyamoya disease: clinical and neuroradiological evaluation. *J Neurosurg* 1984;61:1032-37
- Yamada I, Himeno Y, Suzuki S, et al. Posterior circulation in moyamoya disease: angiographic study. *Radiology* 1995;197:239-46
- Yamada I, Himeno Y, Nagaoka T, et al. Moyamoya disease: evaluation with diffusion-weighted and perfusion echo-planar MR imaging. *Radiology* 1999;212:340-47
- Yamada I, Murata Y, Umehara I, et al. SPECT and MRI evaluations of the posterior circulation in moyamoya disease. *J Nucl Med* 1996;37:1613-17
- Mugikura S, Takahashi S, Higano S, et al. The relationship between cerebral infarction and angiographic characteristics in childhood moyamoya disease. *AJNR Am J Neuroradiol* 1999;20:336-43
- Piao R, Oku N, Kitagawa K, et al. Cerebral hemodynamics and metabolism in adult moyamoya disease: comparison of angiographic collateral circulation. *Ann Nucl Med* 2004;18:115-21
- Taki W, Yonekawa Y, Kobayashi A, et al. Cerebral circulation and metabolism in adults' moyamoya disease: PET study. *Acta Neurochir (Wien)* 1989;100:150-54
- Schumann P, Touzani O, Young AR, et al. Evaluation of the ratio of cerebral blood flow to cerebral blood volume as an index of local cerebral perfusion pressure. *Brain* 1998;121:1369-79
- Mihara F, Kuwabara Y, Tanaka A, et al. Reliability of mean transit time obtained using perfusion-weighted MR imaging: comparison with positron emission tomography. *Magn Reson Imaging* 2003;21:33-39
- Kikuchi K, Murase K, Miki H, et al. Quantitative evaluation of mean transit times obtained with dynamic susceptibility contrast-enhanced MR imaging and with (133)Xe SPECT in occlusive cerebrovascular disease. *AJR Am J Roentgenol* 2002;179:229-35
- Kaneko K, Kuwabara Y, Mihara F, et al. Validation of the CBF, CBV, and MTT values by perfusion MRI in chronic occlusive cerebrovascular disease: a comparison with <sup>15</sup>O-PET. *Acad Radiol* 2004;11:489-97
- Lythgoe DJ, Ostergaard L, William SC, et al. Quantitative perfusion imaging in carotid artery stenosis using dynamic susceptibility contrast-enhanced magnetic resonance imaging. *Magn Reson Imaging* 2000;18:11-11
- Rempp KA, Brix G, Wenz F, et al. Quantification of regional cerebral blood flow and volume with dynamic susceptibility contrast-enhanced MR imaging. *Radiology* 1994;193:637-41
- Sorensen AG, Reimer P. Cerebral MR perfusion imaging: principles and current applications. Stuttgart and New York: Thieme;2000:48-51
- Wirstam R, Anderson L, Ostergaard L, et al. Assessment of regional blood flow by dynamic susceptibility contrast MRI using different deconvolution techniques. *Magn Reson Med* 2000;43:691-700
- Ostergaard L, Weiskoff RM, Chester DA, et al. High resolution measurement of cerebral blood flow using intravascular tracer bolus passages. Part I. Mathematical approach and statistical analysis. *Magn Reson Med* 1996;36:715-25
- Bereczki D, Wei L, Otsuka T, et al. Hypercapnia slightly raises blood volume and sizably elevates flow velocity in brain microvessels. *Am J Physiol* 1993;264:1360-69
- Lin W, Celik A, Derdeyn C, et al. Quantitative measurement of cerebral blood flow in patients with unilateral carotid artery occlusion: a PET and MR study. *J Magn Reson Imaging* 2001;14:659-67
- Hagen T, Bartylla K, Piegras U. Correlation of regional cerebral blood flow measured by stable xenon CT and perfusion MRI. *J Comput Assist Tomogr* 1999;23:257-64
- Kuwabara Y, Ichiya Y, Otsuka M, et al. Cerebral hemodynamic change in the child and the adult with moyamoya disease. *Stroke* 1990;21:272-77
- Kuwabara Y, Ichiya Y, Sasaki M, et al. Cerebral hemodynamics and metabolism in moyamoya disease: a positron emission tomography study. *Clin Neurol Neurosurg* 1997;99(suppl 2):S74-78
- Gibbs JM, Wise RJ, Leenders KL, et al. Evaluation of cerebral perfusion reserve in patients with carotid-artery occlusion. *Lancet* 1984;11:310-14
- Kuwabara Y, Ichiya Y, Sasaki M, et al. Response to hypercapnia in moyamoya disease: cerebrovascular response to hypercapnia in pediatric and adult patients with moyamoya disease. *Stroke* 1997;28:701-707
- Nighoghossian N, Berthezene Y, Philippon B, et al. Hemodynamic parameter assessment with dynamic susceptibility contrast magnetic resonance imaging in unilateral symptomatic internal carotid artery occlusion. *Stroke* 1996;27:474-79
- Nogawa S, Fukuuchi Y, Kobari M, et al. Local cerebral hemodynamic changes through the angiographic stages of moyamoya disease. *Keio J Med* 2000;49(suppl 1):A90-94
- Calamante F, Ganesan V, Kirkham FJ. MR perfusion imaging in Moyamoya syndrome: potential implications for clinical evaluation of occlusive cerebrovascular disease. *Stroke* 2001;32:2810-16